Large increases in emissions of methane and nitrous oxide from eutrophication in Lake Erie

Short title: Methane and nitrous oxide emissions from Lake Erie

Julianne M. Fernandez[1], Amy Townsend-Small*[1], Arthur Zastepa[2], Susan B. Watson[4], and Jay A. Brandes[3]

Affiliations:

[1]Department of Geology, University of Cincinnati, Cincinnati, Ohio, USA.

[2]Environment and Climate Change Canada, Canada Centre for Inland Waters, Burlington, Ontario, Canada.

[3]Skidaway Institute of Oceanography, Savannah, Georgia, USA.

[4]Department of Biology, University of Waterloo, Waterloo Ontario, Canada.

*Corresponding author

E-mail: amy.townsend-small@uc.edu

Abstract

Eutrophication is linked to greenhouse gas emissions from inland waters. Phytoplankton blooms in Lake Erie, one of Earth's largest lakes, have increased with nutrient runoff linked to climate warming, although greenhouse gas emissions from this or other large eutrophic lakes are not well characterized. We measured greenhouse gases around Lake Erie in all four seasons and found that CH_4 and N_2O emissions have increased 10 times or more with re-eutrophication, especially during and after phytoplankton blooms. Lake Erie is a positive source of CH_4 throughout the entire year and around the entire lake, with the highest emissions in spring and summer near the mouth of the Maumee River. While Lake Erie is an overall N_2O source, it is an N_2O sink in winter throughout the lake and in some locations during large phytoplankton blooms. We estimate that Lake Erie emits ~6300 metric tons of CH_4-C yr^{-1} (± 19%) and ~600 metric tons N_2O-N yr^{-1} (± 37%): almost 500,000 metric tons CO_2-eq yr^{-1} total. These results highlight the gravity of eutrophication-related increases in large lake GHG emissions: an overlooked, but potentially major feedback to global climate change.

Introduction

Lake Erie is one of Earth's largest eutrophic lakes, with a history of eutrophication linked to decades of urban, agricultural, and industrial impacts (1). The Great Lakes Water Quality Agreement in 1972 reduced point source nutrient pollution and phytoplankton biomass (2). However, since the mid-1990s, Lake Erie has experienced "re-eutrophication", especially the Western Basin, attributed to a rise in rainfall and non-point source fertilizer runoff from the Maumee River watershed (2)(3). This has led to massive, sometimes toxic, phytoplankton blooms, drinking water intake closures, and exacerbation of central basin hypoxia (3)(4)(5).

Climate change is implicated in water quality declines, as increased intensity and rates of precipitation increases watershed nutrient and sediment inputs (6).

Lakes, rivers, and reservoirs play a major role in the global carbon cycle and greenhouse gas emissions budgets (7–11). Inland waters are a major source of CH_4 globally, and anthropogenic construction of reservoirs enhances this flux (12). Eutrophication leads to CH_4 and N_2O evasion from lakes (13)(14)(10), and eutrophication will increase in lake and coastal ecosystems as runoff and agricultural activity increase globally (6)(15). The greenhouse gases CH_4 and N_2O are 25 and 289 times more powerful than carbon dioxide (CO_2) over 100 year time scales, respectively (16). Despite decades of research on nutrients and phytoplankton in the Great Lakes, there is sparse research on GHGs in Lake Erie (17)(18)(19)(20)(21). However, if increasing eutrophication in Lake Erie linked to climate change leads to increasing emissions of CH_4 and N_2O, this represents a positive feedback that urgently needs to be both delineated and addressed (22).

Lake Erie is the shallowest in average depth (~19 m), has the shortest water residence time, and is the lowest in latitude of the North American Great Lakes (23,24). The lake is divided lengthwise by an international border between the northern United States and the most southern portion of Canada. The lake is also roughly divided into three main basins by depth: the Western Basin, the Central Basin, and the Eastern Basin. The watershed is urbanized, industrialized, and agricultural, with 17 cities in both countries including several industrial hubs (24,25). The main water source into Lake Erie is the upper Great Lakes via the Detroit River (24). Although drilling for oil and gas in the Great Lakes is currently banned in the United States, the Canadian

63 waters of Lake Erie have been actively drilled for natural gas by Canada since the 1930s (18).
64 Currently, there are over 2000 conventional natural gas wells offshore in the Canadian waters of
65 Lake Erie (http://www.ogsrlibrary.com), approximately 500 of which are actively producing.
66 The lake is characterized by high cyanobacteria and phytoplankton biomass, including the
67 harmful cyanobacteria *Microcystis*, in the Western basin (and to a lesser extent, the Central
68 basin), driven by spring and summer nutrient runoff from the Maumee and Sandusky Rivers
69 (2,6). Past research from our research group has indicated Lake Erie is a positive source of CH_4
70 to the atmosphere in the Central Basin in the late summer season (18).

71

72 In order to determine whether Lake Erie is an annual source of CH_4 and N_2O over the entire
73 surface, we carried out CH_4 and N_2O measurements throughout Lake Erie during all four seasons
74 from May 2015 – August 2016, including two mid-summer dates (August 2015 and 2016) and
75 one in winter (February 2016), when the lake had partial ice cover. We also made measurements
76 of CO_2 emissions and sources (using stable isotopes) during August 2016.

77

78 Materials and methods

79 *Sample collection* – Sampling was conducted aboard the Canadian Coast Guard Ship (CCGS)
80 *Limnos* and the CCGS *Griffon*. Water was collected from the Western, Central, and Eastern
81 basin of the lake, with sampling conducted on both sides of the international border. Cruise dates
82 were as follows: 12th - 15th May 2015, 24th - 27th August 2015, 5th - 8th October 2015, 15th - 19th
83 February 2016, and 29th August – 1st September 2016 (Fig 1, Tables S1-S6). A YSI EXO 2
84 Multi-parameter Sonde, equipped with an EXO Conductivity and Temperature Smart Sensor,

85 EXO Optical Dissolved Oxygen Smart Sensor, and a guarded EXO pH Smart Sensor, was
86 deployed at each station for water column profile characteristics.
87
88
89 **Fig. 1**. **Sampling locations and methane (CH_4), nitrous oxide (N_2O), and carbon dioxide**
90 **(CO_2) fluxes in Lake Erie observed over the entire study period.** CH_4 fluxes are shown in the
91 left column and the legend is the same for each month of the study period (mg C m^{-2} d^{-1}). N_2O
92 fluxes are shown in the center column and both positive and negative fluxes are shown (mg N m^{-2}
93 d^{-1}). Positive N_2O fluxes are shown in colors and negative (i.e., N_2O uptake) in white. CO_2
94 fluxes were only measured in August 2016 and are shown in mg C m^{-2} d^{-1}; all CO_2 fluxes were
95 negative at this time. Also shown are the locations of natural gas wells and their status (active,
96 abandoned, suspended, lost, or unknown).
97
98
99 Surface water samples for greenhouse gas (CH_4 and N_2O) analysis were taken at approximately
100 at 1 m depth. Niskin bottles (5 L or 20 L) were used to collect surface water at 1 m depth into
101 155 mL glass serum bottles. Samples were overfilled three times using a tube at the bottom of
102 each bottle to minimize gas loss and atmospheric contamination. Saturated $HgCl_2$ brine (100 µL)
103 was pipetted into the sample for preservation. Samples were sealed with gray butyl rubber septa
104 and an aluminum crimp to minimize exposure to the atmosphere. Greenhouse gas samples were
105 stored at room temperature until analysis.
106

Samples were also taken for pH, alkalinity, and dissolved organic carbon (DIC) concentration and isotopic (δ^{13}C-DIC) analysis in August 2016. Surface water samples for pH analysis were transferred from Niskin bottles into clean 60 mL HDPE bottles as soon as the CTD rosette was brought onboard. These samples were poured into a clean 50 mL beaker with a magnetic stir rod and placed above a stir plate and pH was measured onboard using a Thermoscientific Orion 4-Star pH-Conductivity bench top meter with a refillable Ag/AgCl electrode. Water for alkalinity analysis was collected directly from the Niskin spout into two 60 mL syringes with an attachable 0.45 µm syringe filter. Alkalinity samples were filtered into a clean 125 mL HDPE bottle and either analyzed on ship after room temperature was reached or samples were stored at 4°C for later analysis.

Water samples for δ^{13}C-DIC analysis were collected directly from the Niskin spout into a 30 mL syringe. The water was then filtered with an attachable Puradisc 0.7µm glass microfiber filter and delivered into a 2 mL wide mouth glass autosampler vial through a short 18 g needle. After the sample overflowed into the vial, it was then capped with an 11 mm PTFE rubber septa and crimped shut. The samples were then stored at 4°C.

Sample Analysis – Dissolved gases were extracted from each sample using headspace extraction methods. At room temperature, 30 mL of ultra-high purity N_2 was injected into a water sample in a serum vial, and 30 mL of water displaced into a second syringe, which created an inert headspace within the sample bottle. The bottles were then agitated for one minute with a Fisher Scientific Multi-Tube Vortexer to release any dissolved gases. As the 30 mL of displaced water was placed back into the sample bottle, a 30 mL syringe was used to extract the released gases

130 from the headspace. The headspace gas was then transferred into a previously evacuated glass
131 vial containing desiccant beads that was sealed with a butyl rubber septum and aluminum crimp
132 cap. These headspace samples were analyzed using a Shimadzu Scientific Instruments Gas
133 Chromatograph (GC)-2014 Greenhouse Gas Analyzer equipped with a flame ionization detector
134 (FID) and an electron capture detector (ECD) at the University of Cincinnati.

135

136 Calibrated greenhouse gas standards were placed intermittently throughout the sample run to
137 generate a calibration curve. Concentrations of calibrated CH_4 standards range from 2.18 to
138 1,000 ppm in air (n = 4) and N_2O standards range from 293 to 393 ppb (n = 3). The original
139 dissolved gas concentrations in the water samples were determined with the temperature-specific
140 Bunsen solubility coefficients (18) using the measured headspace gas concentrations. The
141 equilibrium dissolved gas concentrations were calculated using water temperature, barometric
142 pressure, and monthly average background atmospheric CH_4 and N_2O concentrations at the
143 Mauna Loa Observatory during the time of sampling (28,29). Variation in final dissolved
144 greenhouse gas concentration is about 6% using headspace extraction in our laboratory (13,14).

145

146 Alkalinity was measured by acid titration using a HACH Digital titrator equipped with sulfuric
147 acid (0.16 N) and using a Thermoscientific Orion 4-Star pH-Conductivity bench top with a
148 refillable Ag/AgCl electrode to record the inflection points. The recorded pH, acid count, and
149 temperatures were entered into the USGS Alkalinity Calculator version 2.22 (30), which
150 analyzes the titration curve and calculates the alkalinity using an acid correction factor of 1.01
151 and the inflection point method. DIC concentration and δ^{13}C-DIC were measured via isotope
152 ratio mass spectrometry at Skidaway Institute of Oceanography via the method of (31).

153

154 *Surface Flux Analysis* – Surface fluxes of CH_4 and N_2O were calculated for all of the sampling
155 periods using the following equation:

156 $$F = k (C_w - C_{sat}) \quad (1)$$

157 Where F is the flux, k is the gas transfer velocity, C_w is the measured CH_4 or N_2O concentration
158 in surface water (measured as described above), and C_{sat} is the calculated equilibrium
159 concentration of atmospheric CH_4 or N_2O in surface water (calculated as described above) (32).
160 The gas transfer velocity (k) is calculated with the average wind speed and corresponding
161 temperature dependent freshwater Schmidt number (33). Wind speed was averaged from the
162 Port Stanley buoy, station 45132, for the duration of each sampling period
163 (https://www.ndbc.noaa.gov/station_page.php?station=45132) (usually one week).

164

165 CO_2 surface fluxes were calculated via USGS CO_2-calc v4.0.9 (34). Measured values of pH,
166 alkalinity, water temperature and average wind speed during sampling periods were used as the
167 primary variables. Flux velocity is determined as a function of the average wind speed, and a
168 Schmidt number of 600 was used for freshwater at 20°C (33). The CO_2 constants (K_1, K_2, and
169 K_w) (35) and pressure effects (36) were chosen accordingly for freshwater. CO_2 fluxes for each
170 site (in August 2016 only) are shown in Table S6.

171

172 *Scaling Up* – We categorized each site visited during each sampling trip to the Western, Central,
173 or Eastern basin of Lake Erie based on its location within the lake and lake bathymetry (23)
174 (Tables S1-S5). We then calculated monthly average CH_4 and N_2O emission rates for each basin
175 for February, May, August (for each year and using an average of both 2015 and 2016 data), and

October (Table S7 and S8). We then multiplied the average emission rate for each basin and each month by the surface area of each basin (Western basin = 3,284 km^2; Central basin = 16,138 km^2; Eastern basin = 6,235 km^2), multiplied by the number of days in each month, and added up the emissions from each basin to get a monthly total (Tables S9 and S10). We used the average 2015 and 2016 emission rates for August for final calculations. Finally, we used linear interpolation to scale between measurement months to estimate an annual total for both CH_4 and N_2O (Fig S1).

Error Estimation – To estimate the range in monthly and annual CH_4 and N_2O emissions, we calculated an average percent error for each gas. For each basin of the lake and each sampling month, we calculated the standard error of the average emission rate of CH_4 or N_2O (the standard deviation divided by the square root of the number of measurements). We then converted this to a percent error by dividing the standard error by the emission rate for that month. We calculated an average percent error for each basin and each gas, and then averaged each of those to estimate an average error for the emission measurement for CH_4 and N_2O, respectively. This method assumes that the largest source of variability in emission rates is differences within basins, and not measurement uncertainties – which are small compared to the spatial and temporal variability we observed in fluxes. The average percent error for CH_4 was 19% and the average percent error for N_2O was 37%. For some months, such as May 2015 in the Western Basin, we observed simultaneous high N_2O fluxes in the Maumee River mouth and negative N_2O fluxes elsewhere in the Western Basin, which leads to higher error estimates for N_2O as compared to CH_4. We also observed both negative and positive N_2O fluxes in the Central Basin in May 2015 and August 2016.

Results and discussion

Methane – We found positive emissions of CH_4 throughout the lake all year, including February (Fig 1). The highest CH_4 emissions were in spring and summer, and from the shallow (Z_{max} ~10 m) (37) Western Basin (Figs 1 and 2). Emissions were lower in the deeper Central Basin, despite summer stratification, anoxia, and previous reports of CH_4 buildup in the hypolimnion (18). The highest CH_4 emissions from Lake Erie are similar to those from thawing permafrost lakes and ponds in the Arctic (38); however, unlike in Arctic lakes, we found low under-ice CH_4 concentrations and emissions in winter (Figs 1 and 2).

Fig. 2. Basin-wide average CH_4 (left) and N_2O (right) fluxes for each month of measurements in the study. Also shown are separate averages for August 2015 and 2016 and both August trips together (Aug 2015 & 2016). Error bars represent standard error. CH_4 plot shows separate columns for the Central Basin of Canada and US, as natural gas drilling is permitted in Canadian waters only.

Methane was previously measured in the Western Basin of Lake Erie in late summer 1969, near the Lake Erie islands (17)(39). The 1969 emission rate was 0.5 mg C m^{-2} d^{-1}, ~10 times lower than our measurement from approximately the same location in August 2015 (site 478, 4.6 mg C

220 m^{-2} d^{-1}; Table S2) (17)(39). These data suggest that CH_4 emissions from Western Lake Erie have
221 increased. The (17) reference concluded that "methane…must be considered in the total cycle of
222 carbon in this eutrophic lake" (17). Despite this important observation, however, no further
223 measures of CH_4 were published until our recent study in 2016.

224

225 Contrary to our previous work using stable isotopes (18), the current data do not indicate that
226 natural gas production is a major source of CH_4 in Lake Erie, for several reasons. In the current
227 study, we measured CH_4 emissions in winter, when temperature-dependent biological CH_4
228 production is expected to be lowest, and found no significant difference between CH_4 emissions
229 in the Central and Eastern basin over gas wells (average flux = 0.05 ± 0.004 mg C m^{-2} d^{-1}) versus
230 those not (0.04 ± 0.003 mg C m^{-2} d^{-1}). We also found no difference in δ^{13}C-DIC or DIC
231 concentration in samples taken in bottom waters in August 2016 in over gas wells versus non-gas
232 producing areas (see further discussion below). Furthermore, the current study showed that the
233 majority of CH_4 emissions were largely found in the Western Basin, not sampled in our previous
234 study, where there are no gas wells (Fig 1). Emissions of CH_4 from the Western Basin are most
235 likely derived from biogenic CH_4 production in sediments. Finally, we note that most wells in
236 Lake Erie are plugged and not producing natural gas, and thus would not be expected to be a
237 large CH_4 source (40).

238

239 A recent study reported CH_4 concentrations and isotopic composition of CH_4 in Lake Michigan
240 and Lake Superior from June 2017 (21). Methane concentrations in summer in Lake Erie were
241 more than 200 times higher than in Lake Superior (21) (Table S1). Surface water CH_4
242 concentrations ranged from 3.5 to 60 nM in Lakes Michigan and Superior (21), much lower than

in Lake Erie, where concentrations in May 2015 (the closest sampling month to June) ranged from 14 to 780 nM (Table S1). The highest CH_4 concentrations in (21) were found in coastal Lake Michigan where the highest primary production rates are found, and the highest sediment methanogenesis rates are likely (21), similar to the current study. As we also concluded in the current study, radiocarbon measurements indicated no input of CH_4 from old sources, such as fossil fuels (21), although radiocarbon measurements of CH_4 in Lake Erie would help further indicate the relative inputs of natural gas and biogenic CH_4 in active production areas.

Nitrous Oxide – N_2O emissions showed different spatial and temporal patterns than CH_4 (Figs. 1 and 2). This is not surprising, as CH_4 is likely produced in anoxic sediments whereas N_2O production and consumption occur under both aerobic and anaerobic conditions in sediments and the water column (41). The highest N_2O emissions were in the Central Basin in August 2015 (Fig 1). N_2O emissions also differed between the two August sampling trips (Figs 1 and 2): in the north-central basin, higher emissions were observed in 2015 than in August 2016, when a phytoplankton bloom likely reduced dissolved N concentrations and therefore nitrification. We also observed some negative N_2O fluxes in the Central and Western Basin in May 2015 and August 2016, and throughout the lake in February 2016 (Figs 1 and 2).

There are no recent studies of N_2O in Lake Erie. In August 1977, a negative N_2O flux was measured near the mouth of the Detroit River (19), in comparison to our fluxes of 0.4 mg N m^{-2} d^{-1} in August 2015 (site 881; Table S2) and 0.02 mg N m^{-2} d^{-1} in August 2016 (site 971; Table S5) in the same area (Fig. 1). N_2O emissions have increased in Lake Erie: indeed, our data indicate that western Lake Erie has flipped from an overall sink to a source of N_2O along with re-

266 eutrophication. Eutrophic lakes are not currently considered a source of anthropogenic N_2O in
267 global budgets (42), although recent studies suggest their emission rate is globally significant
268 (10).

269

270 Nitrous oxide uptake has been documented previously in eutrophic reservoirs and agricultural
271 lakes. A recent study of eutrophic agricultural reservoirs in the Great Plains of Canada found
272 widespread undersaturation and uptake of N_2O (43). A study of a eutrophic reservoir near
273 Cincinnati, Ohio found that denitrification consumed N_2O at some periods during the year
274 although it was an N_2O source on annual time scales (13). Overall, there are less studies that
275 have included N_2O than CH_4 in eutrophic lakes and reservoirs (43), and these studies indicate
276 that more measurements are needed to elucidate the role of N_2O in an increasingly warmer,
277 wetter, and nutrient enriched world.

278

279 *Carbon Dioxide* – Carbon dioxide emission rates were only measured in August 2016, and all
280 fluxes were negative, reflecting high photosynthesis and/or low respiration (Fig 1). Methane
281 oxidation contributes to the dissolved inorganic C pool. Methane is ^{13}C-depleted relative to CO_2
282 (44); we observed lower $\delta^{13}C$-DIC concentrations at sites with higher DIC and CH_4
283 concentrations in bottom waters throughout Lake Erie (Fig. 3, Table S6), indicating a greater
284 presence of DIC from CH_4 oxidation in samples with high DIC (Fig 3). There was no difference
285 in $\delta^{13}C$-DIC in sites with and without gas wells, indicating biogenic CH_4 is the predominant
286 source of CH_4 in Lake Erie (Fig 3), in contrast to our previous study (18). These data indicate
287 that if positive CO_2 emissions occur later in the season, the production of CH_4 in the lake due to
288 eutrophication may enhance biogenic CO_2 emissions. CO_2 is a large contributor to the GHG

289 footprint of other large eutrophic lakes (10). However, it is unknown whether Lake Erie is a net
290 sink or source for CO_2 on annual time scales (45)(46), and thus whether it contributes to
291 increasing atmospheric CO_2 and climate warming. The current and predicted CO_2 balance of
292 large lakes such as Lake Erie is a critical data gap that should be targeted by future work (47).

293

294

295 **Fig 3. Carbon isotopic composition ($\delta^{13}C$ [‰; VPDB]) of dissolved inorganic carbon (DIC)**
296 **versus the DIC concentration (left) and the CH_4 concentration (right)**. All data are from
297 samples taken 1 m from the bottom sediments. Samples taken proximal to and away from
298 natural gas wells are indicated.

299

300

301 *Scaling Up* – CH_4 and N_2O emissions occur most in spring, summer, and fall in Lake Erie (Fig.
302 2), and most in the Western Basin (particularly for CH_4), corresponding with highest seasonal
303 phytoplankton biomass (May-October; (2)). We estimate annual emissions from Lake Erie of
304 6,294 ± 1,259 metric tons CH_4-C yr^{-1} and 597 ± 209 metric tons N_2O-N yr^{-1}, or 209,775 metric
305 tons CO_2-equivalent (CO_2-e) for CH_4 and 279,286 metric tons CO_2-e for N_2O (16)(48). This is
306 the equivalent of over 100,000 cars driven for one year, or almost 250 million kilograms of coal
307 burned in a year (48).

308

309 We compared our results to data published by USEPA on CH_4 emissions in the Great Lakes
310 region from large facilities in the waste, oil and natural gas, and fertilizer production sectors (49).

311 This showed that Lake Erie emits CH_4 at a rate comparable to and higher than most landfills and
312 natural gas distribution systems in the US states of Ohio and Michigan. By way of comparison,
313 in 2017 over 200 facilities reported emissions in Ohio, and only three landfills, one natural gas
314 distribution company, and one fertilizer plant had CH_4 emissions greater than our annual
315 estimate for Lake Erie, while in Michigan fewer than six of the 200+ facilities reporting CH_4
316 exceeded those of Lake Erie. Furthermore, Lake Erie represented a larger N_2O source than any
317 other industrial source in Ohio or Michigan reported to EPA in 2017, although, fertilized
318 agricultural soils, the largest anthropogenic N_2O source regionally and nationally (42), do not
319 appear in this database.

320

321 Conclusions

322 We present a new and significant observation on the negative effects of phytoplankton blooms in
323 Lake Erie. If climate change and eutrophication increase CH_4 and N_2O emissions from Lake
324 Erie, as indicated here and elsewhere (10)(22)(11), this represents a positive feedback to climate
325 warming. A warmer and wetter climate may lead to higher CH_4 and N_2O emissions from Lake
326 Erie, particularly with increasing nutrient inputs. Carbon cycle-climate change feedbacks are the
327 main driver of interannual variability and increases in global CH_4 concentrations (42)(50). A
328 growing body of evidence also shows that eutrophic water bodies such as Lake Erie also
329 contribute to the global N_2O budget with a positive feedback to climate warming (42). These
330 results also have significant implications for other inland waters and imply that greenhouse gas
331 emissions from eutrophic lakes – particularly large ones – should be considered for inclusion in
332 anthropogenic greenhouse gas budgets, as these represent regionally significant fluxes.

Acknowledgments

The authors thank F. Åkerström, C. Botner, D. Disbennett, A. Fries, and K. Jimenez for laboratory assistance; J. Beaulieu, R. Bourbonierre, M. Griffin, and C. Winslow for helpful discussions while designing this study; and the captain and crew of the *CCGS Limnos* and the *CCGS Griffon* for sampling assistance and for keeping us alive and supplied with poutine during research cruises. **Author contributions:** J.M.F. and A.T.S. designed the study and interpreted results with input from all authors; J.M.F. collected the samples and analyzed them for CH_4, N_2O, and CO_2; J.A.B. analyzed samples for DIC and DIC isotopes; and J.M.F. and A.T.S. wrote the paper with contributions from all authors. **Data and materials availability:** All data and methods needed to reproduce the results in the paper are provided in the supporting information.

References

1. Egan D. The Death and Life of the Great Lakes. Vol. 1. W.W. Norton & Company, Inc.; 2017. 384 p.

2. Kane DD, Conroy JD, Peter Richards R, Baker DB, Culver DA. Re-eutrophication of Lake Erie: Correlations between tributary nutrient loads and phytoplankton biomass. Journal of Great Lakes Research. 2014 Sep 1;40(3):496–501.

3. Watson SB, Miller C, Arhonditsis G, Boyer GL, Carmichael W, Charlton MN, et al. The re-eutrophication of Lake Erie: Harmful algal blooms and hypoxia. Harmful Algae. 2016 Jun 1;56:44–66.

4. Scavia D, David Allan J, Arend KK, Bartell S, Beletsky D, Bosch NS, et al. Assessing and addressing the re-eutrophication of Lake Erie: Central basin hypoxia. Journal of Great Lakes Research. 2014 Jun 1;40(2):226–46.

5. Steffen MM, Davis TW, McKay RML, Bullerjahn GS, Krausfeldt LE, Stough JMA, et al. Ecophysiological Examination of the Lake Erie Microcystis Bloom in 2014: Linkages

between Biology and the Water Supply Shutdown of Toledo, OH. Environ Sci Technol. 2017 Jun 20;51(12):6745–55.

6. Michalak AM, Anderson EJ, Beletsky D, Boland S, Bosch NS, Bridgeman TB, et al. Record-setting algal bloom in Lake Erie caused by agricultural and meteorological trends consistent with expected future conditions. PNAS. 2013 Apr 16;110(16):6448–52.

7. Cole JJ, Prairie YT, Caraco NF, McDowell WH, Tranvik LJ, Striegl RG, et al. Plumbing the Global Carbon Cycle: Integrating Inland Waters into the Terrestrial Carbon Budget. Ecosystems. 2007 Feb 1;10(1):172–85.

8. Bastviken D, Tranvik LJ, Downing JA, Crill PM, Enrich-Prast A. Freshwater Methane Emissions Offset the Continental Carbon Sink. Science. 2011 Jan 7;331(6013):50–50.

9. Tranvik LJ, Downing JA, Cotner JB, Loiselle SA, Striegl RG, Ballatore TJ, et al. Lakes and reservoirs as regulators of carbon cycling and climate. Limnology and Oceanography. 2009;54(6part2):2298–314.

10. DelSontro T, Beaulieu JJ, Downing JA. Greenhouse gas emissions from lakes and impoundments: Upscaling in the face of global change. Limnology and Oceanography Letters. 2018;3(3):64–75.

11. Deemer BR, Harrison JA, Li S, Beaulieu JJ, DelSontro T, Barros N, et al. Greenhouse Gas Emissions from Reservoir Water Surfaces: A New Global Synthesis. BioScience. 2016 Nov 1;66(11):949–64.

12. Saunois M, Bousquet P, Poulter B, Peregon A, Ciais P, Canadell JG, et al. The global methane budget 2000–2012. Earth System Science Data. 2016 Dec 12;8(2):697–751.

13. Beaulieu JJ, Smolenski RL, Nietch CT, Townsend-Small A, Elovitz MS, Schubauer-Berigan JP. Denitrification alternates between a source and sink of nitrous oxide in the hypolimnion of a thermally stratified reservoir. Limnology and Oceanography. 2014;59(2):495–506.

14. Beaulieu JJ, Smolenski RL, Nietch CT, Townsend-Small A, Elovitz MS. High Methane Emissions from a Midlatitude Reservoir Draining an Agricultural Watershed. Environ Sci Technol. 2014 Oct 7;48(19):11100–8.

15. Sinha E, Michalak AM, Balaji V. Eutrophication will increase during the 21st century as a result of precipitation changes. Science. 2017 Jul 28;357(6349):405–8.

16. United States Environmental Protection Agency. Inventory of U.S. Greenhouse Gas Emissions and Sinks 1990-2016 [Internet]. 2018. Available from: https://www.epa.gov/ghgemissions/inventory-us-greenhouse-gas-emissions-and-sinks-1990-2016

17. Howard DL, Frea JI, Pfister RM. The potential for methane carbon cycling in Lake Erie. 14th Conference on Great Lakes Research, International Association of Great Lakes Research; 1977; Ann Arbor, Michigan.

18. Townsend-Small A, Disbennett D, Fernandez JM, Ransohoff RW, Mackay R, Bourbonniere RA. Quantifying emissions of methane derived from anaerobic organic matter respiration and natural gas extraction in Lake Erie. Limnology and Oceanography. 2016;61(S1):S356–66.

19. Lemon E, Lemon D. Nitrous oxide in fresh waters of the Great Lakes Basin1. Limnology and Oceanography. 1981;26(5):867–79.

20. Ouyang Z, Shao C, Chu H, Becker R, Bridgeman T, Stepien CA, et al. The Effect of Algal Blooms on Carbon Emissions in Western Lake Erie: An Integration of Remote Sensing and Eddy Covariance Measurements. Remote Sensing. 2017 Jan;9(1):44.

21. Joung D, Leonte M, Kessler JD. Methane sources in the waters of Lake Michigan and Lake Superior as revealed by natural radiocarbon measurements. Geophysical Research Letters [Internet]. [cited 2019 May 14];0(ja). Available from: https://agupubs.onlinelibrary.wiley.com/doi/abs/10.1029/2019GL082531

22. Beaulieu JJ, DelSontro T, Downing JA. Eutrophication will increase methane emissions from lakes and impoundments during the 21st century. Nature Communications. 2019 Mar 26;10(1):1375.

23. Bolsenga SJ, Hernendorf CE. Lake Erie and Lake St. Clair Handbook. Detroit, Michigan, USA: Wayne State University Press; 1993. 467 p.

24. Hartig JH, Zarull MA, Ciborowski JJH, Gannon JE, Wilke E, Norwood G, et al. Long-term ecosystem monitoring and assessment of the Detroit River and Western Lake Erie. Environ Monit Assess. 2009 Nov;158(1–4):87–104.

25. Waples JT, Eadie B, Klump JV, Squires M, Cotner J, McKinley G. The Laurentian Great Lakes. North American continental margins: A synthesis and planning workshop Report of the North American continental margins working group for the US carbon cycle scientific steering group and interagency working group US Carbon Cycle Science Program (B Hales, WJ Cai, BG Mitchell, CL Sabine, and O Schofield [eds]). 2008;73–81.

26. Yamamoto S, Alcauskas JB, Crozier TE. Solubility of methane in distilled water and seawater. J Chem Eng Data. 1976 Jan 1;21(1):78–80.

27. Weiss RF, Price BA. Nitrous oxide solubility in water and seawater. Marine Chemistry. 1980 Feb 1;8(4):347–59.

28. Dlugokencky EJ, Crotwell AM, Lang PM, Mund JW, Rhodes ME. Atmospheric Methane Dry Air Mole Fractions from quasi-continuous measurements at Barrow, Alaska and Mauna Loa, Hawaii, 1986-2017, Version 2018-03-19 [Internet]. 2017. Available from: Path: ftp://aftp.cmdl.noaa.gov/data/trace_gases/ch4/in-situ/surface/

29. Elkins JW, Nance D, Hall B. Nitrous oxide data from the NOAA/ESRL halocarbons in situ program [Internet]. NOAA National Centers for Environmental Information; 2017 [cited

2019 May 14]. Available from: https://data.nodc.noaa.gov/cgi-bin/iso?id=gov.noaa.ncdc:C01556

30. Rounds SA. Alkalinity calculator, version 2.22 [Internet]. Oregon Water Science Center, U.S. Geological Survey; 2013. Available from: https://or.water.usgs.gov/alk/index.html

31. Brandes JA. Rapid and precise δ13C measurement of dissolved inorganic carbon in natural waters using liquid chromatography coupled to an isotope-ratio mass spectrometer. Limnology and Oceanography: Methods. 2009;7(11):730–9.

32. Bender ML, Kinter S, Cassar N, Wanninkhof R. Evaluating gas transfer velocity parameterizations using upper ocean radon distributions. Journal of Geophysical Research: Oceans [Internet]. 2011 [cited 2019 Feb 28];116(C2). Available from: https://agupubs.onlinelibrary.wiley.com/doi/abs/10.1029/2009JC005805

33. Wanninkhof R. Relationship between wind speed and gas exchange over the ocean. Journal of Geophysical Research: Oceans. 1992;97(C5):7373–82.

34. Robbins LL, Hansen ME, Kleypas JA, Meylan SC. CO2calc: A User-Friendly Seawater Carbon Calculator for Windows, Mac OS X, and iOS (iPhone) [Internet]. 2010 [cited 2019 Feb 28] p. 17. Report No.: USGS Open-File Report 2010-1280. Available from: https://pubs.usgs.gov/of/2010/1280/

35. Millero FJ. The thermodynamics of the carbonate system in seawater. Geochimica et Cosmochimica Acta. 1979 Oct 1;43(10):1651–61.

36. Millero FJ. CHAPTER 43 - Influence of Pressure on Chemical Processes in the Sea. In: Riley JP, Chester R, editors. Chemical Oceanography [Internet]. Academic Press; 1983 [cited 2019 Feb 28]. p. 1–88. Available from: http://www.sciencedirect.com/science/article/pii/B9780125886086500079

37. National Oceanic and Atmospheric Administration, National Centers for Environmental Information. Bathymetry of Lake Erie and Lake St. Clair [Internet]. 2018. Available from: https://www.ngdc.noaa.gov/mgg/greatlakes/erie.html

38. Townsend-Small A, Åkerström F, Arp CD, Hinkel KM. Spatial and Temporal Variation in Methane Concentrations, Fluxes, and Sources in Lakes in Arctic Alaska. Journal of Geophysical Research: Biogeosciences. 2017;122(11):2966–81.

39. Bastviken D, Cole J, Pace M, Tranvik L. Methane emissions from lakes: Dependence of lake characteristics, two regional assessments, and a global estimate. Global Biogeochemical Cycles [Internet]. 2004 [cited 2019 Feb 28];18(4). Available from: https://agupubs.onlinelibrary.wiley.com/doi/abs/10.1029/2004GB002238

40. Townsend-Small A, Ferrara TW, Lyon DR, Fries AE, Lamb BK. Emissions of coalbed and natural gas methane from abandoned oil and gas wells in the United States. Geophysical Research Letters. 2016;43(5):2283–90.

468 41. Townsend-Small A, Prokopenko MG, Berelson WM. Nitrous oxide cycling in the water
469 column and sediments of the oxygen minimum zone, eastern subtropical North Pacific,
470 Southern California, and Northern Mexico (23°N–34°N). Journal of Geophysical Research:
471 Oceans. 2014;119(5):3158–70.

472 42. Ciais P, Sabine C, Bala G, Bopp L, Brovkin V, Canadell J, et al. Carbon and Other
473 Biogeochemical Cycles. In: Climate Change 2013: The Physical Science Basis
474 Contribution of Working Group I to the Fifth Assessment Report of the Intergovernmental
475 Panel on Climate Change [Stocker, TF, D Qin, G-K Plattner, M Tignor, SK Allen, J
476 Boschung, A Nauels, Y Xia, V Bex and PM Midgley (eds)]. Cambridge, United Kingdom
477 and New York, NY, USA: Cambridge University Press; 2013. p. 106.

478 43. Webb JR, Hayes NM, Simpson GL, Leavitt PR, Baulch HM, Finlay K. Widespread nitrous
479 oxide undersaturation in farm waterbodies creates an unexpected greenhouse gas sink. Proc
480 Natl Acad Sci USA. 2019 Apr 29;201820389.

481 44. Whiticar MJ. Carbon and hydrogen isotope systematics of bacterial formation and oxidation
482 of methane. Chemical Geology. 1999 Sep 30;161(1):291–314.

483 45. McKinley G, Urban N, Bennington V, Pilcher D, McDonald C. Preliminary Carbon Budgets
484 for the Laurentian Great Lakes. 2011;24.

485 46. Phillips JC, McKinley G, Bennington V, Bootsma H, Pilcher D, Sterner R, et al. The
486 Potential for CO2-Induced Acidification in Freshwater: A Great Lakes Case Study.
487 Oceanography. 2015 Jun 1;25(2):136–45.

488 47. Benway HM, Alin SR, Boyer E, Cai W-J, Coble PG, Cross JN, et al. A science plan for
489 carbon cycle research in North American coastal waters. Report of the Coastal CARbon
490 Synthesis (CCARS) community workshop, August 19-21, 2014 [Internet]. Woods Hole,
491 MA: cean Carbon and Biogeochemistry Program; 2016 [cited 2019 Apr 9]. Available from:
492 https://hdl.handle.net/1912/7777.2

493 48. US EPA. Greenhouse Gas Equivalencies Calculator [Internet]. US EPA. 2018 [cited 2019
494 Mar 2]. Available from: https://www.epa.gov/energy/greenhouse-gas-equivalencies-
495 calculator

496 49. EPA Greenhouse Gas Reporting Program [Internet]. 2017. Available from:
497 www.epa.gov/ghgreporting

498 50. Nisbet EG, Dlugokencky EJ, Manning MR, Lowry D, Fisher RE, France JL, et al. Rising
499 atmospheric methane: 2007–2014 growth and isotopic shift. Global Biogeochemical
500 Cycles. 2016;30(9):1356–70.

501

502

Supporting Information

Table S1. May 2015 Lake Erie dissolved [CH_4] and [N_2O] and surface fluxes. CCGS Limnos cruise dates were May 12th - 14th 2015. Data from water collected 1 meter below the surface water and atmosphere interface. Average windspeed was 4.73 m s^{-1}. Sample locations are shown in Figure 1.

Table S2. August 2015 Lake Erie dissolved [CH_4] and [N_2O] and surface fluxes. CCGS Limnos cruise dates were August 24th - 27th 2015. Data from water collected 1 meter below the surface water and atmosphere interface. Average windspeed was 6.65 m s^{-1}. Sample locations are shown in Figure 1.

Table S3. October 2015 Lake Erie dissolved [CH_4] and [N_2O] and surface fluxes. CCGS Limnos cruise dates were October 5th - 8th 2015. Data from water collected 1 meter below the surface water and atmosphere interface. Average windspeed was 3.84 m s^{-1}. Sample locations are shown in Figure 1.

Table S4. February 2016 Lake Erie dissolved [CH_4] and [N_2O] and surface fluxes. CCGS Griffon cruise dates were February 15th - 19th 2016. Data from water collected 1 meter below the surface water and atmosphere interface. Average windspeed was 1.97 m s^{-1}. Sample locations are shown in Figure 1.

Table S5. August 2016 Lake Erie dissolved [CH_4] and [N_2O] and surface fluxes. CCGS Limnos cruise dates were August 29th to September 1st 2016. Data from water collected 1 meter below the surface water and atmosphere interface. Average windspeed was 4.05 m s^{-1}. Sample locations are shown in Figure 1.

Table S6. August 2016 Lake Erie [DIC], ^{13}C-DIC, [CO_2], CO_2 surface flux and relevant sample information. CCGS Limnos cruise dates were August 29th to September 1st 2016. Data from water collected 1 meter below the surface water and atmosphere interface, and from 1 m from the sediment water interface. Average windspeed was 4.05 m s^{-1}. DIC concentration and ^{13}C-DIC was determined via isotope ratio mass spectrometry at Skidaway Institute of Oceanography via the method of Brandes (2009). Sample locations are shown in Figure 1.

Table S7. Monthly average CH_4 surface fluxes for each basin of Lake Erie.

Table S8. Monthly average N_2O surface fluxes for each basin of Lake Erie.

Table S9. Weighted average CH_4 flux of each sampling month of the whole lake. The daily average flux is multiplied by the surface area (Bolsenga and Herdenforf, 1993) of the designated basin for an estimate of the total flux of the basin. The sum of all the basins for each sampling period is the estimated daily flux of the whole lake. Multiplying the lake total by the number of days in the sampling month estimates the total flux for the month.

Table S10. The weighted average N_2O flux of each sampling month of the whole lake. The daily average flux is multiplied by the surface area (Bolsenga and Herdenforf, 1993) of the designated basin for an estimate of the total flux of the basin. The sum of all the basins for each sampling period is the estimated daily flux of the whole lake. Multiplying the lake total by the number of days in the sampling month estimates the total flux for the month.

Table S11. Average annual CH_4 and N_2O surface flux. A monthly average was produced for the months that were not measured by calculating the linear regression between each measured month and then applying this regression to the months between. The annual total for both CH_4 and N_2O is the sum of the calculated and estimated values for a full year. These measurements and estimates are also shown in Figure S1.

Fig. S1. Annual trends in average lake-wide emissions of CH_4 (left) and N_2O (right). The larger points on each curve represent months when measurements were made (Fig. 1), and smaller points are estimated using linear extrapolation as described in the methods. The lake is a positive source of CH_4 all year, and a weak sink for N_2O in winter, but fluxes of both gases are highest in late summer. Annual emissions were estimated by summing both measured and estimated monthly fluxes. For a discussion of error estimates, please see the supplemental methods.

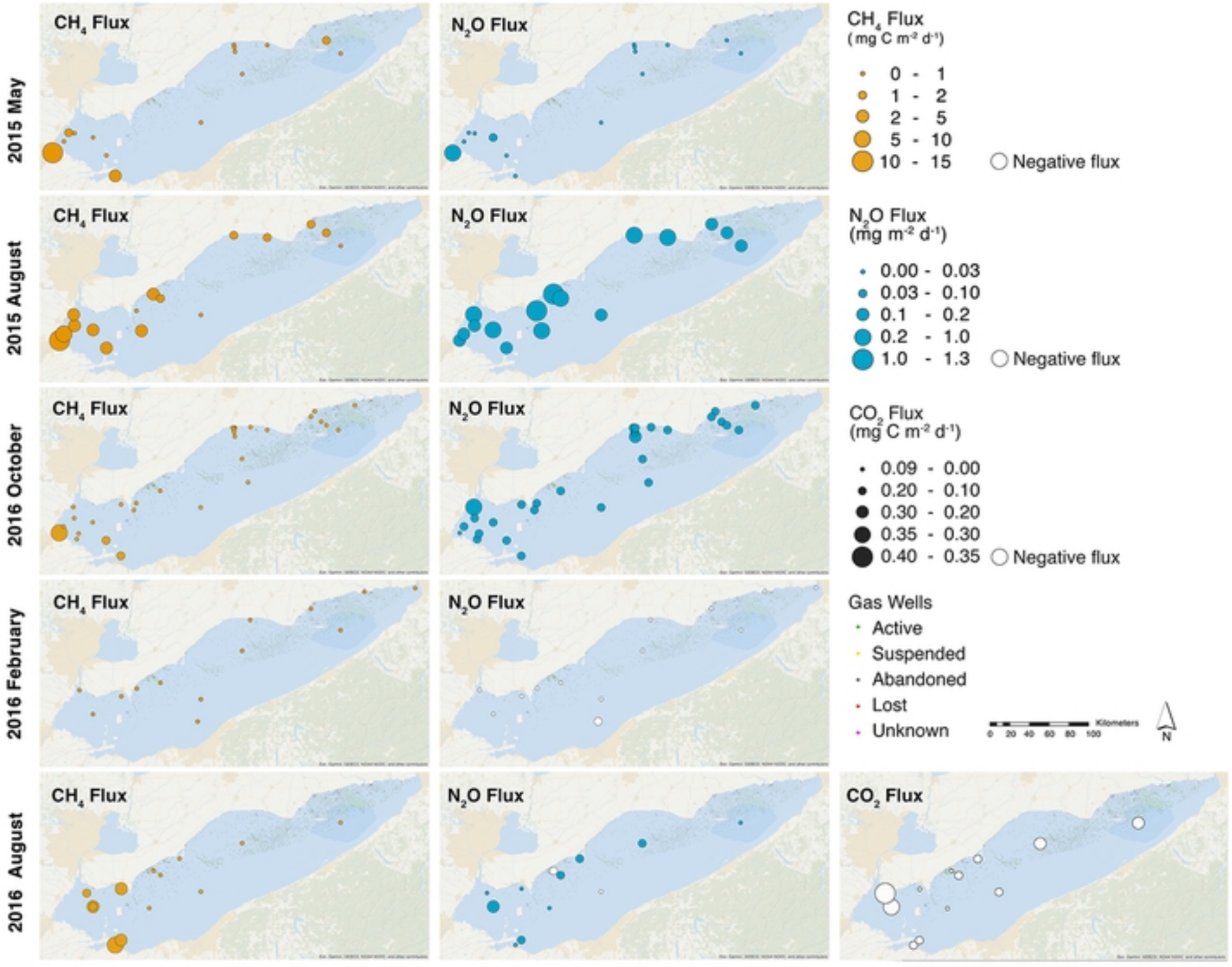
2015 May
2015 August
2016 October
2016 February
2016 August
CH4 Flux
N2O Flux
CO2 Flux
CH4 Flux
(mg C m-2 d-1)
0 - 1
1 - 2
2 - 5
5 - 10
10 - 15
Negative flux
N2O Flux
(mg m-2 d-1)
0.00 - 0.03
0.03 - 0.10
0.1 - 0.2
0.2 - 1.0
1.0 - 1.3
Negative flux
CO2 Flux
(mg C m-2 d-1)
0.09 - 0.00
0.20 - 0.10
0.30 - 0.20
0.35 - 0.30
0.40 - 0.35
Negative flux
Gas Wells
Active
Suspended
Abandoned
Lost
Unknown
Kilometers
0 20 40 60 80 100
N

figure 1

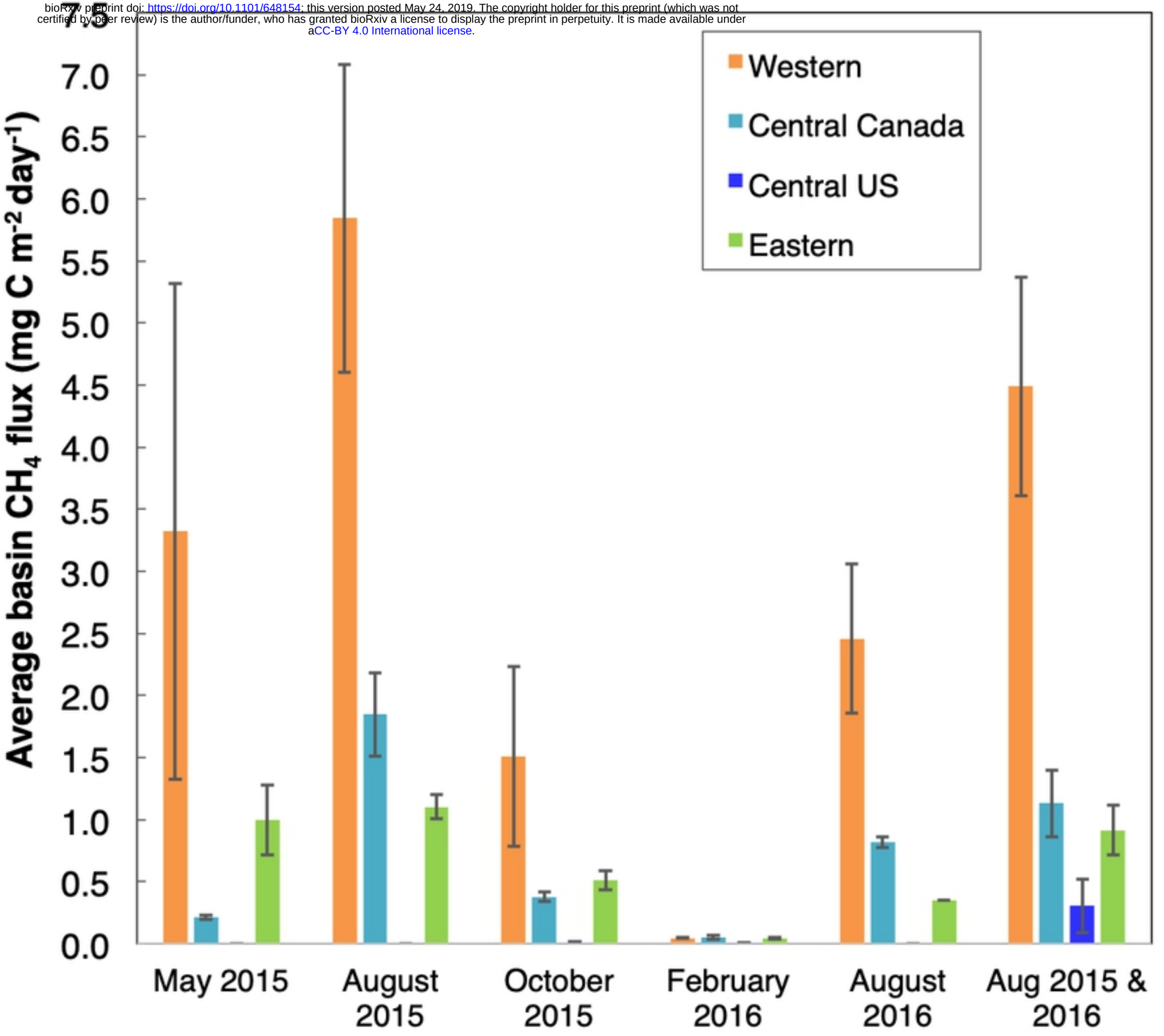

figure 2a

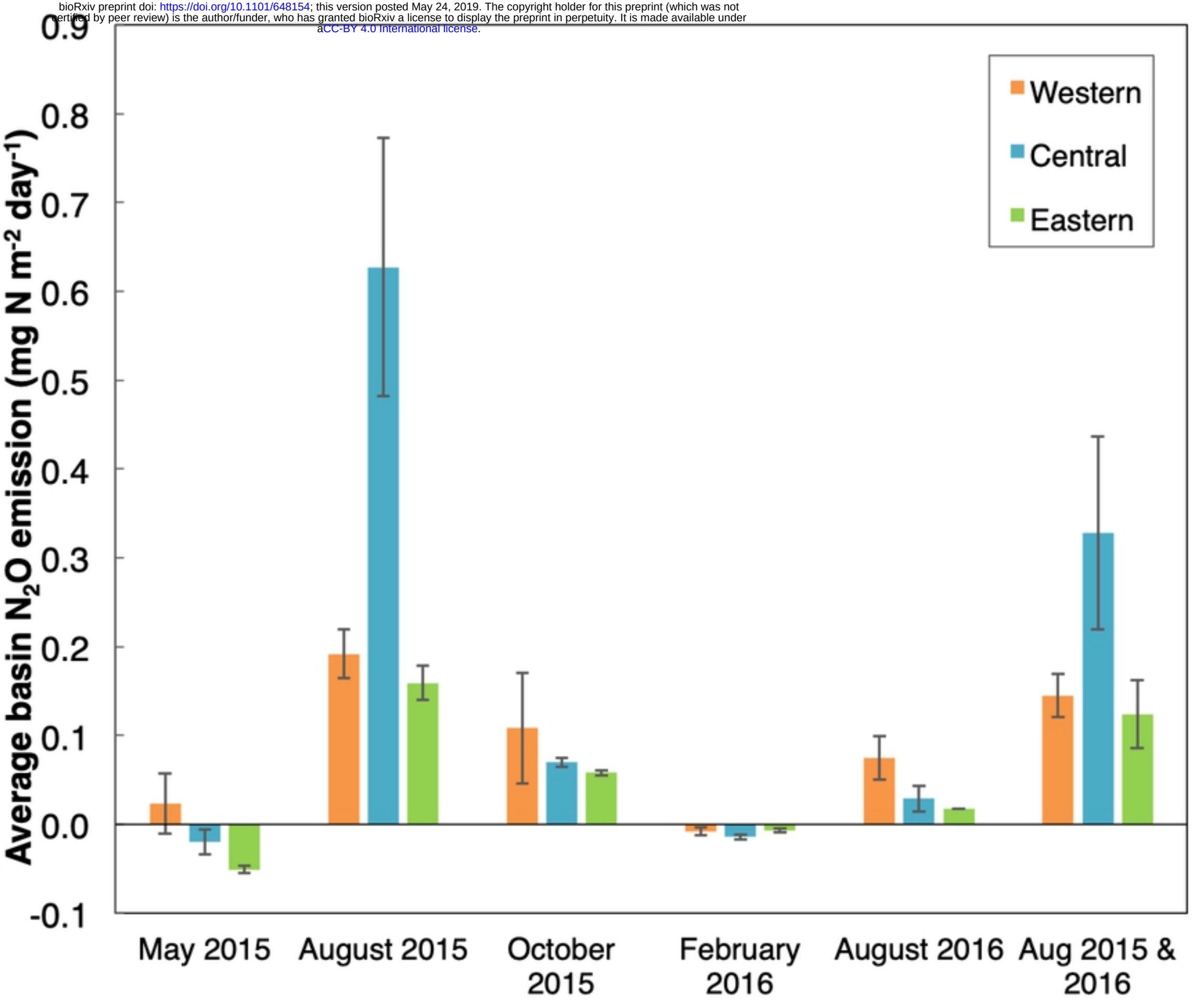

figure 2b

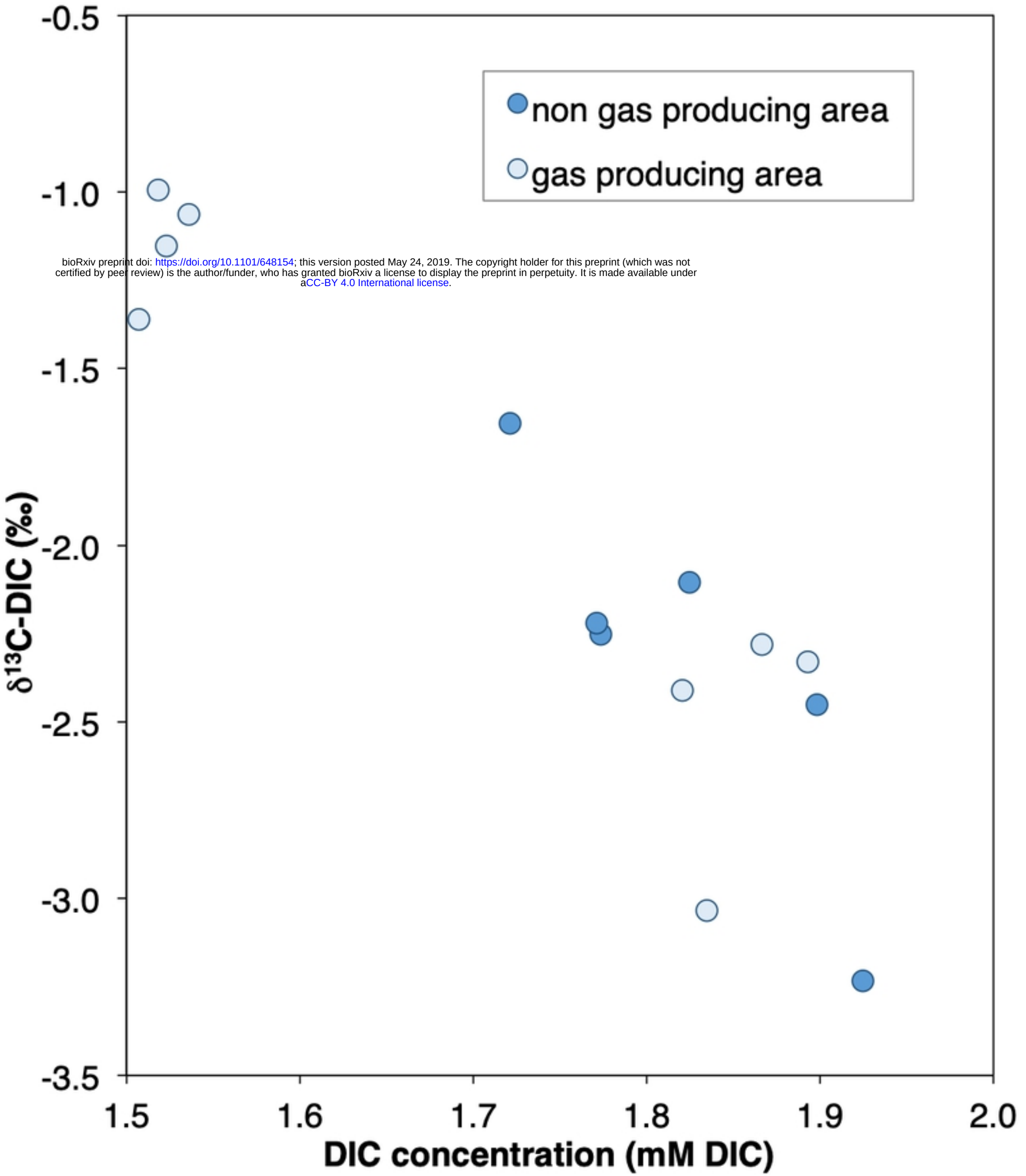

figure 3a

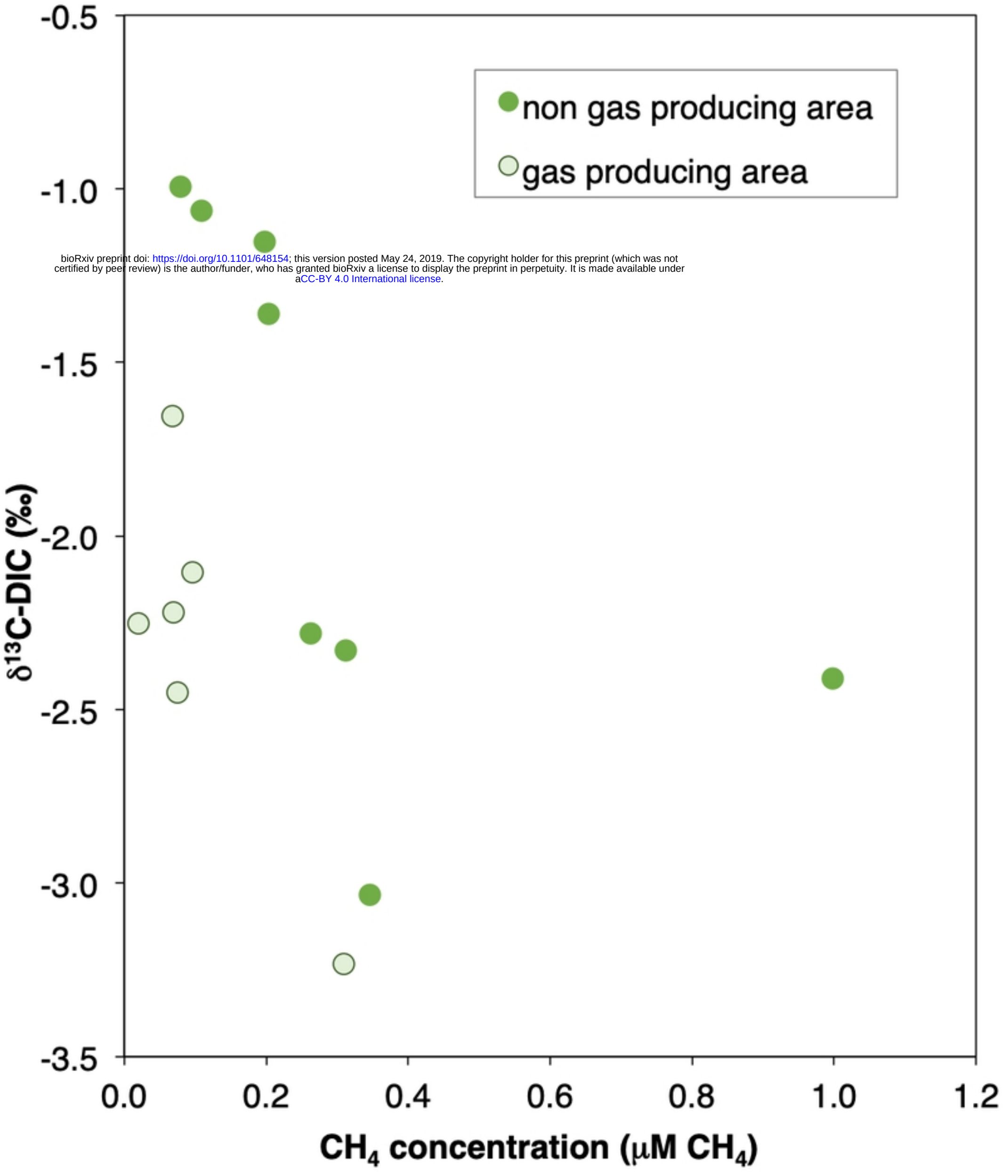

figure 3b